Chemical Engineering Journal 163 (2010) 28–34

Contents lists available at ScienceDirect

Chemical Engineering Journal

journal homepage: www.elsevier.com/locate/cej

Azo dye degradation kinetics in TiO_2 film-coated photoreactor

Pei-Jen Lu, Cheng-Wei Chien, Tai-Shang Chen, Jia-Ming Chern *

Department of Chemical Engineering, Tatung University,40 Chungshan North Road, 3rd Sec., Taipei, 10451, Taiwan

ARTICLE INFO

Article history:
Received 21 January 2010
Received in revised form 4 June 2010
Accepted 12 July 2010

Keywords:
Dye degradation
Kinetics
Modeling
TiO_2 film

ABSTRACT

In this study, commercial nano-size TiO_2 suspension was used to coat on the inner surface of glass reactors and the immobilized TiO_2 film served as photocatalyst to decompose azo dye in aqueous solutions. A full factorial design approach using three factors, namely rotation time, rotation speed, and drying temperature was adopted to prepare TiO_2-coated reactors. The azo dye decomposition conversion under 8 W UV illumination for 4 h was measured as the response of the experimental design. The results showed that the three main effects were significant: increasing the rotation time from 10 to 50 min leaded to 11.4% increase in the dye conversion; increasing the rotation speed from 10 to 50 rpm leaded to 5.6% increase in the dye conversion; increasing the drying temperature from 150 to 250 °C leaded to 2.8% increase in the dye conversion. A series of dye degradation experiments with varying initial dye concentrations were conducted using the TiO_2-coated reactor. The dye degradation rate was found to be $-r_{dye} = k_a C/(1 + k_b C)$ with $k = 0.0326\ min^{-1}$ and $k_b = 0.764\ L\ mg^{-1}$. The developed kinetic model was used to fit the experimental data satisfactorily.

1. Introduction

The presence of dyes in the effluents produced by textile industrial processes leads to colorful contamination. In addition to containing toxic and hazardous pollutants, the colorful wastewater is aesthetically unacceptable. Therefore, the treatment of textile wastewater has received increasing attention. A variety of methods for pollutant removal and decolourization of textile wastewaters are available [1]. Although most textile wastewater treatment plants use biological treatment processes to remove BOD and COD, most dyes cannot be completely biodegraded by the conventional biological wastewater treatment processes. In order to meet more increasingly stringent environmental regulations and laws, tertiary treatment such as adsorption or chemical oxidation is required after the biological treatment processes to remove the residual dye and color.

The most widely tertiary treatment for dye wastewater was adsorption by activated carbon or other low cost materials [2–7]. Due to the difficulty of regenerating dye-saturated activated carbon or other adsorbents, chemical oxidation, especially advanced oxidation process (AOP) employing hydroxyl radicals to degrade dyes becomes an attractive choice for dye wastewater treatment. There are several methods for generating hydroxyl radicals, e.g. Fenton and Fenton-based processes [8–10], ozonation and ozone-based processes [11,12], UV irradiation and UV-based processes [13–18], electrochemical methods [19–22], and photocatalysts [23–25].

Using TiO_2 suspension under UV irradiation is one of the simplest AOPs for dye degradation [26], but the problem is how to separate TiO_2 particles from the reaction solution after dye degradation. To overcome the TiO_2 separation problem, TiO_2 immobilization technique became very important and received great attention. Many techniques such as spray pyrolysis, chemical vapor deposition, microwave synthesis, vacuum arc plasma evaporation, spin coating–pyrolysis, and sol–gel process have been used to prepare TiO_2 thin films on various substrates [27–41]. The coated TiO_2 thin films were characterized and tested for their effectiveness as photocatalysts for organics removal. The above preparation methods need delicate equipment and the operating costs are expensive. Therefore, this study aimed at coating commercially available nano TiO_2 sol on the inside surface of glass reactors for azo dye degradation by a simple and inexpensive method. The factorial experimental design methodology was adopted to study how the rotation speed, rotation time, and drying temperature affected the TiO_2 film performance quantified by the dye removal rate at the same degradation condition. Furthermore, the TiO_2-coated glass reactor prepared under the optimal condition was used to study the dye degradation kinetics.

2. Experimental

2.1. Materials

The acid HNO_3 (Shou Pin Chemicals Co., LTD., Japan) and base NaOH (Nihon Shyaku Ind., LTD., Japan) were used for pretreating the

* Corresponding author. Tel.: +886 2 25925252x2561x123; fax: +886 2 25861939.
E-mail address: jmchern@ttu.edu.tw (J.-M. Chern).

1385-8947/$ – see front matter © 2010 Elsevier B.V. All rights reserved.
doi:10.1016/j.cej.2010.07.022

Table 1
The properties of TiO_2 suspension.

Parameter	Value	Unit
Crystallite size	5	nm
Anatase	100	%
pH-value	Approximate 1	
Solids content	15.2	%
Density	1.12	g cm^{-3}
Nitrate content	2.0	%

inner surfaces of the glass reactors. The properties of the commercial nano-sized TiO_2 suspension (Hombikat XXS100, Sachtleben Chemie Gmbh, Germany) are shown in Table 1. The peach red azo dye (Sumitomo Chemical Co., Japan) with main ingredient of triphenyalmethane shown in Fig. 1 was used to prepare the synthetic wastewater in this study.

2.2. Preparation and characterization of TiO_2 film

A glass reactor with inside diameter of 6 cm and height 25 cm was coated with TiO_2 film by the procedure described as follows. The glass reactor was first washed with 0.1N NaOH solution for 30 min and rinsed with deionized water. It was washed with 0.1N nitric acid and rinsed with deionized water. After drying the glass reactor at the room temperature, 100 mL nano-sized TiO_2 suspension was charged to the glass reactor. Then the glass reactor was put horizontally in a rotation machine for film coating as schematically shown in Fig. 2. The motor was controlled at a desired rotation speed to coat the inner surface of the glass reactor uniformly with the TiO_2 suspension. Before the motor rotation started, the inner surface of the bottom half of the glass reactor immersed in the TiO_2 suspension and thus some TiO_2 sol adhered on the inner surface of the glass reactor. Once the TiO_2 sol-wetted surface left the TiO_2 suspension during the motor rotation, the solvent in the TiO_2 sol-wetted surface evaporated and thin TiO_2 film appeared. The development of the TiO_2 film during the above coating process is schematically shown in Fig. 3.

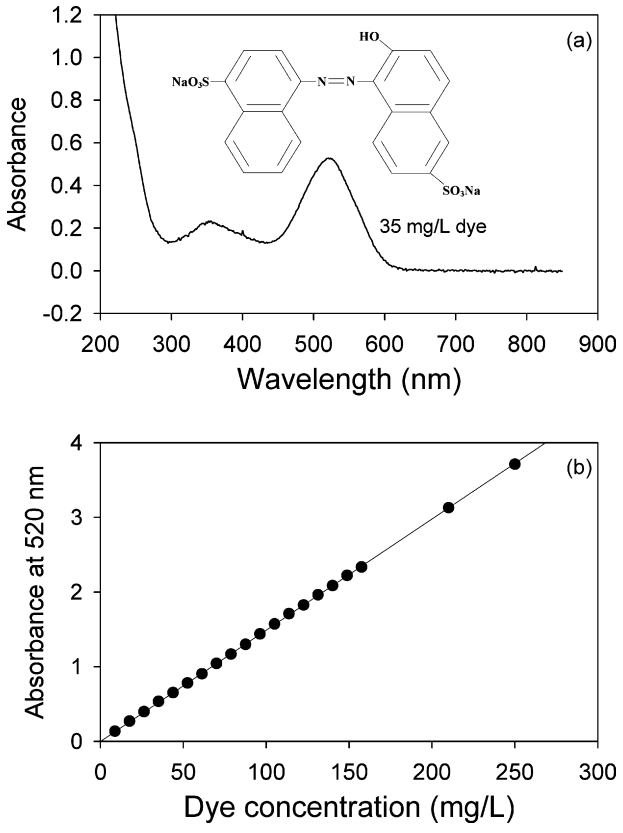

Fig. 1. UV/vis absorbance spectrum and calibration curve of dye aqueous solutions.

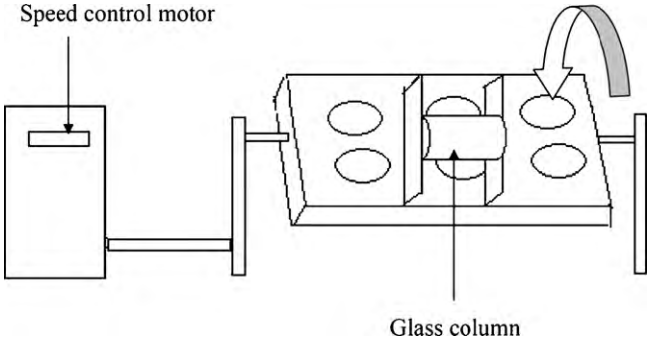

Fig. 2. Schematic diagram of the coating experimental apparatus.

After a period of rotation time, the coated glass reactor with "wet" TiO_2 film was put in an oven with desired temperature set-point and heating rate of 10 °C min^{-1} for 1 h after reaching the desired temperature to allow deposition of TiO_2 film on the inside surface of the glass reactor. Then the glass reactor was taken out of the oven and cooled down to the room temperature. To make sure that the coated TiO_2 film was not stripped off, the glass reactor was washed by deionized water in an ultrasonic chamber for 5 h.

One of the TiO_2 film-coated glass reactors was cracked and the TiO_2 film thickness on the glass pieces was measured by a profilometer (KLA-Tencor, model AlphaStep 200) to be 120 nm. The radiation absorption spectrum measured by a UV–vis spectrophotometer (Jasco, model UV-560) showed characteristic absorption peak between 280 and 360 nm. The TiO_2 film thickness controlled by the rotation speed and time is one of the major factors to determine the photocatalytic reaction rates. If the coated film is too thin, it may be stripped off the glass surface during the irradiation reaction. But if the coated film is too thick, it may reduce the UV light penetration and lower the dye decomposition efficiency. The other important factor is the stickiness of the TiO_2 film onto the glass surface that is mainly dependent on the drying temperature. Therefore we selected the rotation speed, rotation time, and the drying temperature as the three factors for the experimental design. The experimental conditions are summarized in Table 2.

2.3. Photocatalytic degradation of dye solution

The schematic diagram of the photoreactor apparatus is shown in Fig. 4. The glass reactor coated with TiO_2 film was placed vertically in a constant-temperature water bath (model D-630, Deng Yng, Taiwan). 500 mL dye solution with desired initial dye concentration and pH was charged to the glass reactor equipped with a 365 nm, 8 W UV lamp (model FL8BLB, Sankyo, Japan), a magnetic stirrer (Mirak S72725, Barnstead Thermolyne, USA), and a pH meter (Meter Lab PHM 240, Radiometer Co.). The UV lamp with quartz tube diameter of 1.8 cm and length of 26.5 cm was located at the center of the TiO_2 film-coated reactor with 6 cm inside diameter. The length of the UV lamp immersed in the dye solution was about 18 cm. After turning on the UV lamp, the dye solution was pumped through a UV/vis spectrometer (Jasco, UV-560) at different time intervals to measure the dye absorbance at its wavelength of maximum absorbance (520 nm). The dye concentration was calculated by a calibration curve based on the Lambert–Beer's law, as shown in Fig. 1.

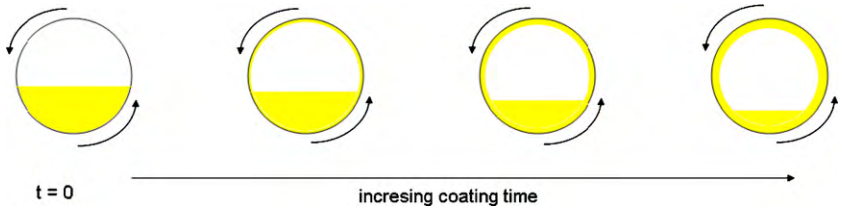

Fig. 3. Development of the wet TiO_2 film during coating process.

Table 2
The experimental conditions and results for the factorial design.

Design no.	Rotation time, X_1 (min)	Rotation speed, X_2 (rpm)	Drying temperature (°C)	Dye removal rate in 4 h[a]
1	10	10	150	72.2%, 74.0%
2	50	10	150	81.4%, 78.5%
3	10	50	150	70.7%, 72.9%
4	50	50	150	81.0%, 79.2%
5	10	10	250	62.0%, 62.8%
6	50	10	250	84.5%, 83.4%
7	10	50	250	80.8%, 80.0%
8	50	50	250	89.7%, 88.6%
9	30	30	200	77.5%, 78.0%

[a] Reaction conditions in the photoreactor: agitation speed = 600 rpm, pH = 5.5, initial dye concen. = 10 mg L^{-1}, temp. = 35 °C.

3. Results and discussion

3.1. Preliminary tests

Four preliminary tests using different experimental conditions were carried out first to make sure that the dye degradation was mainly due to the photocatalytic reaction. The results of the preliminary tests are shown in Fig. 5. The dye concentration remained unchanged in an uncoated reactor in the absence of UV irradiation. After 4-h contact, the dye concentration decreased about 1% in a TiO_2 film-coated reactor in the absence of UV irradiation. This suggests a weak adsorption of the dye molecules on the TiO_2 film. After 4-h UV irradiation in an uncoated reactor, the dye concentration decreased about 4%. This indicates that the dye degradation by the UV irradiation only is also relatively unimportant. Obviously, the dye removal rate under UV irradiation in a TiO_2 film-coated reactor is much greater than those in the other cases. Therefore, the reduction of dye concentration was primarily caused by the photocatalytic reaction occurring on the inner surface coated with TiO_2 film.

3.2. Full factorial design

The response of factorial experimental design can depend on the individual variables and/or the interactions among the variables of consideration. In order to make sure the experimental results were reproducible, two glass columns were coated with the TiO_2 film under replicate conditions. For each glass column, four repeated dye degradation tests were performed and the average of the dye removal rates was treated as the response of the full factorial design. The range of the dye removal rates of the four repeated tests for each glass column was less than 1.5%. This indicates that the TiO_2-coated glass reactor can be repeatedly used for dye degradation. The results of the replicated 2^3 full factorial design are also shown in Table 2. The general mathematical model employed for the 2^3 full factorial design is

$$Y = a_0 + a_1X_1 + a_2X_2 + a_3X_3 + a_{12}X_1X_2 + a_{13}X_1X_3 + a_{23}X_2X_3 + a_{123}X_1X_2X_3 \quad (1)$$

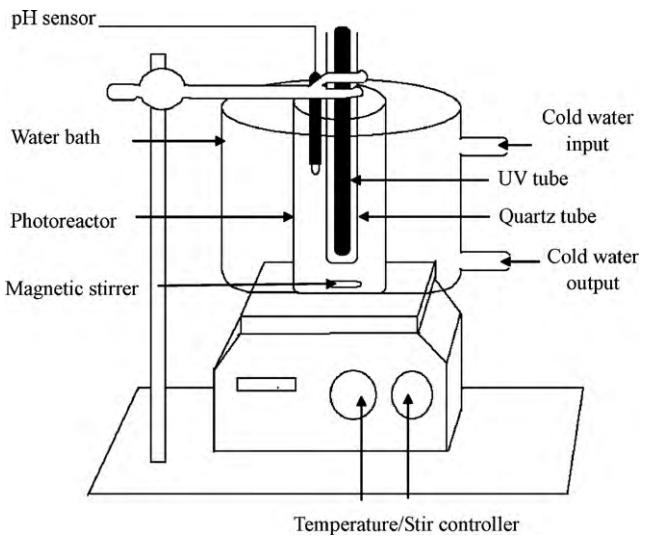

Fig. 4. Schematic diagram of the photoreactor apparatus.

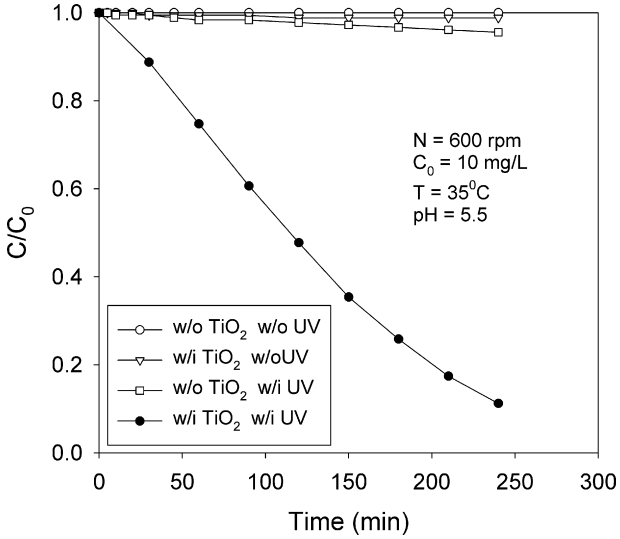

Fig. 5. The preliminary test results.

where a_i is the regression coefficient and X_i is the dimensionless variable defined as:

$$\begin{cases} X_1 = 0.05\ (\text{rotation time}) - 1.5 \\ X_2 = 0.05\,(\text{rotation speed}) - 1.5 \\ X_3 = 0.02\,(\text{drying temperature}) - 4 \end{cases} \quad (2)$$

In Eq. (1), not all the terms are significant. The significant factors in the regression model can be determined by performing an analysis of variance [42]. The sums of squares used to estimate the effects of the factors and the F distribution which is the distribution of the ratio of respective mean-square effect and mean-square error are shown in Table 3. A p-value is a measure of how much evidence we have against the null hypothesis (H_0). The smaller the p-value, the more evidence we have against H_0 and it is also a measurement of how likely we are to obtain a confident model result assuming H_0 is true.

In order to determine the important effects on the dye removal rate, the F distribution and p-value tests were employed. The model F-value of 18.45 shown in Table 3 implies the model is significant. There is only less than 0.01% chance that a model F-value this large could occur due to noise. Values of p less than 0.05 indicate model terms are significant. In this case X_1, X_2, X_{13}, X_{23} are significant model terms. Values of p greater than 0.1 indicate the model terms are not significant. Although the p-value of X_3 suggests that X_3 is not significant, X_3 must be included in the final model because the binary interaction effects X_{13} and X_{23} are significant. Based on the F test and p-value test shown in Table 3, some insignificant effects can be discarded, because these effects do not offer any statistical significance. The final model for the dye removal rate obtained from the above statistical analysis becomes:

$$Y = 0.776 + 0.057X_1 + 0.028X_2 + 0.014X_3 + 0.019X_1X_3 + 0.030X_2X_3 \quad (3)$$

with the significant three main effects and the interactions between the rotation time and drying temperature, and the rotation speed and drying temperature.

In addition to the ANOVA shown in Table 3, the selected model, Eq. (3) can be validated by normal probability plots. The normal probability plot of the effects is shown in Fig. 6a. The effects of a_{12} and a_{123} close to the straight line can be neglected, whereas the others far from the line will be the significant effects [42]. Eq. (3) can be used to predict the dye removal rate for 4 h reaction using varying preparation conditions. We defined the errors as the differences between the predicted removal rates and the experimental removal rates. A normal probability of these errors is shown in Fig. 6b with the root mean square being 2.43%. All the errors scattering around the straight line indicates that the chosen model is a reasonable one [42]. Two separate experiments employed the central point of the design were carried out and the dye removal rates were found to be 77.5% and 78.0%, respectively. These two additional test results re-confirm that the chosen model without quadratic terms is adequate.

The binary interaction plots are shown in Fig. 7. As shown in Fig. 7a, the dye removal rate slightly decreases with increasing drying temperature at the shorter rotation time while it significantly increases with increasing drying temperature at the longer rotation time. As shown in Fig. 7b, the dye removal rate decreases with increasing drying temperature at the lower rotation speed while it increases with increasing drying temperature at the higher rotation speed. For a longer rotation time or a rotation speed, the TiO_2 film coating is thicker so that a higher drying temperature is required to immobilize the film. A thicker immobilized TiO_2 film provides more active sites to catalyze the dye degradation under irradiation of UV light. Among the different preparation conditions of the full factorial design, the optimal condition for the TiO_2 film prepara-

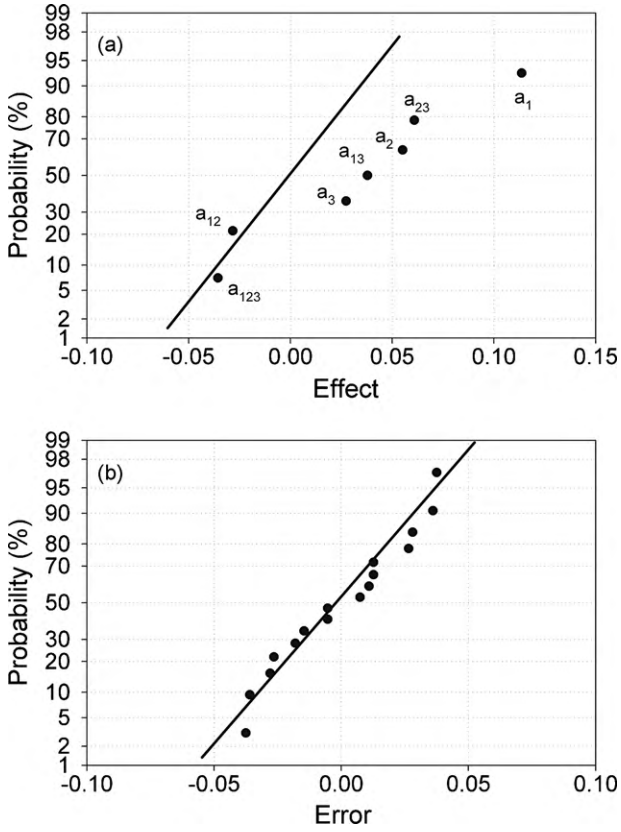

Fig. 6. Normal probability plots of the effects and errors in the factorial design.

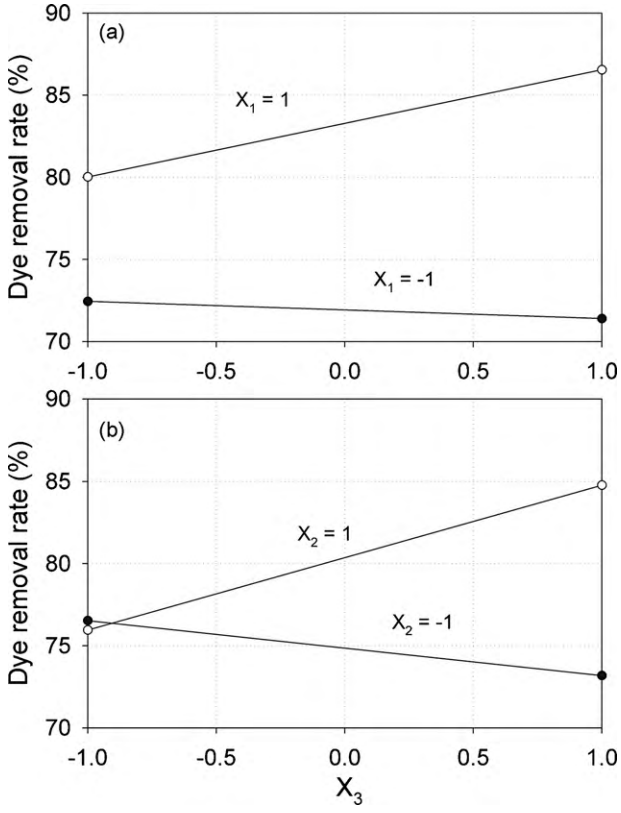

Fig. 7. The binary interaction plots: (a) interaction between rotation time and drying temperature and (b) interaction between rotation speed and drying temperature.

Table 3
Analysis of variance of the dye removal factorial design.[a].

Source	Sum of squares	Degrees of freedom	Mean square	*F*-value	*p*-Value	a_i Coefficient
Model	0.0874	5	0.017471	18.45	<0.0001	0.776
X_1	0.0516	1	0.051643	54.54	<0.0001	0.0568
X_2	0.0122	1	0.012155	12.84	0.0050	0.0276
X_3	2.998E−03	1	0.002998	3.17	0.1056	0.0137
X_{13}	5.738E−03	1	0.005738	6.06	0.0336	0.0189
X_{23}	1.482E−02	1	0.014823	15.65	0.0027	0.0304
Residual	9.469E−03	10	0.000947			
Cor total	0.0968	15				

[a] Obtained from Design Expert 6.07 (Stat-Ease).

tion is: rotation time = 50 min, rotation speed = 50 rpm, and drying temperature = 250 °C as shown in Table 2. We therefore used the optimal conditions to prepare the TiO_2-coated photoreactors for the kinetic experiments.

3.3. Dye degradation kinetics

The experimental results of dye degradation at different agitation speeds, shown in Fig. 8, indicate that the mass transfer effect on the dye degradation kinetics is negligible for the agitation speed greater than 600 rpm. A series of kinetic experiments was performed using constant agitation speed 600 rpm and initial pH 5.5 at 35 °C, but varying initial dye concentrations. The experimental results are shown in Fig. 9. As is shown in Fig. 9, the prevailing first-order kinetic model is not suitable to describe the experimental data of this study. For first-order reactions in batch reactors,

$$\frac{dC}{dt} = -kC \tag{4}$$

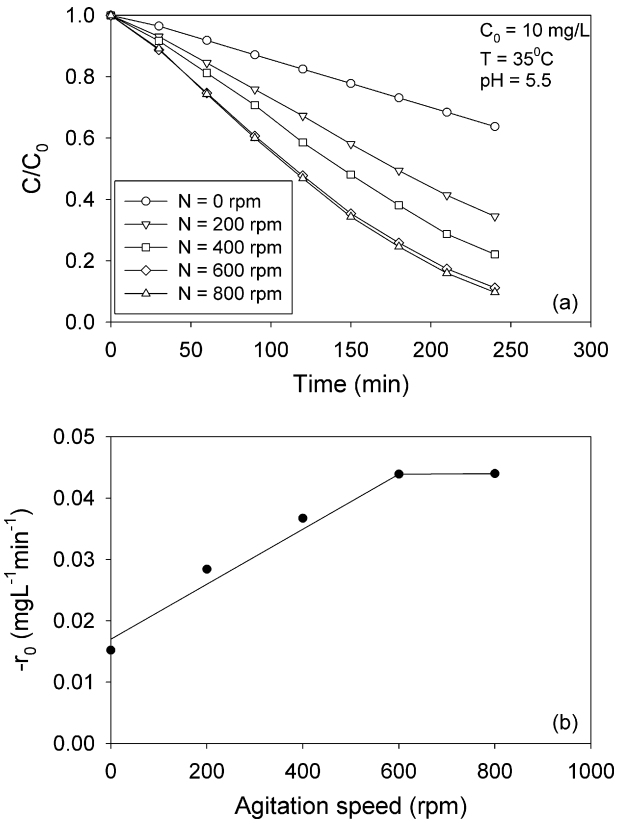

Fig. 8. Effect of agitation speed on the dye degradation rate.

Integrating Eq. (4) with initial condition: at $t = 0$, $C = C_0$ leads to

$$\frac{C}{C_0} = \exp(-k \cdot t) \tag{5}$$

Eq. (5) suggests that the fractional residual concentration of first-order reactions decays exponentially with time only and is independent of the initial reactant concentrations [43]. The strong dependence of the fractional residual concentration on the initial dye concentration, shown in Fig. 9, proves that the dye degradation kinetics is not first order with respect to the dye concentration. Since the first-order kinetic model is not adequate to describe the kinetic data, a new kinetic model is required.

3.4. Reaction mechanism and kinetic model

The simplest reaction mechanism of photocatalyzed dye degradation proposed from considering the reaction steps reported in the literature [44–46] is as follows:

$$TiO_2 + h\nu\ (\lambda < 390\,nm) \underset{k_{10}}{\overset{k_{01}}{\leftrightarrow}} TiO_2\ (h^+) + TiO_2\,(e^-) \tag{6}$$

$$TiO_2\,(h^+) + H_2O \xrightarrow{k_{12}} H^+ + TiO_2\ (^\bullet OH) \tag{7}$$

$$TiO_2\,(e^-) + O_2 \xrightarrow{k_{12'}} TiO_2\,(O_2^{-\bullet}) \tag{8}$$

$$TiO_2\,(^\bullet OH) + dye \xrightarrow{k_{23}} Products + TiO_2 \tag{9}$$

$$TiO_2\ (O_2^{-\bullet}) + dye \xrightarrow{k_{23'}} Products + TiO_2 \tag{10}$$

This proposed mechanism starts with the photocatalyst irradiation by UV light, followed by the formation of hydroxyl radical

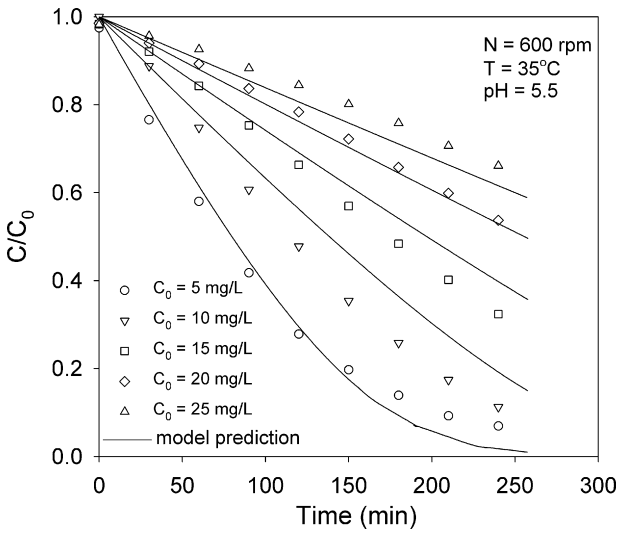

Fig. 9. Experimental and predicted kinetic curves of dye degradation.

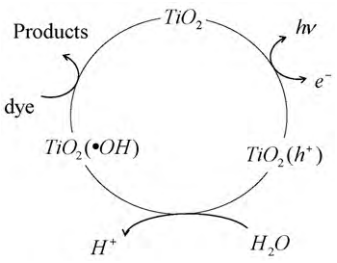

Fig. 10. Reaction network of dye degradation catalyzed by TiO_2 film.

and superoxide radical. The hydroxyl radical and superoxide radical then attack the dye compound as shown in reactions (9) and (10), respectively. Three dye degradation tests using 600 rpm agitation, aeration by pure oxygen, and aeration by pure nitrogen, respectively, were performed and the resultant fractional residual concentration versus time curves almost overlapped. This suggests that reaction steps involving reactions (8) and (10) are less important than those involving the hydroxyl radical steps. If the reaction pathway involving reactions (8) and (10) is neglected, the reaction network according to the proposed mechanism becomes a 3-member single-cycle network as shown in Fig. 10. Without assuming which reaction step is the rate-determining step of the overall reaction, the general rate equation of single-cycle networks [47] can be applied to obtain the following explicit rate equation.

$$-r_{\text{dye}} = -\frac{dC}{dt} = \frac{k_{01}k_{12}k_{23}IC[S_T]}{D_{00} + D_{11} + D_{22}} \tag{11}$$

where the denominator terms can be readily obtained from the following linear pathway segments:

$$D_{00}: \text{TiO}_2 \underset{k_{10}}{\overset{k_{01}\ h\nu}{\longleftrightarrow}} \text{TiO}_2(\text{h}^+) \overset{k_{12}\text{H}_2\text{O}}{\underset{\text{H}^+}{\Longrightarrow}} \text{TiO}_2(^{\bullet}\text{OH}) \underset{\text{Products}}{\overset{k_{23}\ \text{dye}}{\longrightarrow}} \text{TiO}_2\ D_{00}$$
$$= k_{12}k_{23}C + k_{10}k_{23}C \tag{12}$$

$$D_{11}: \text{TiO}_2\ (\text{h}^+) \overset{k_{12}\text{H}_2\text{O}}{\underset{\text{H}^+}{\Longrightarrow}} \text{TiO}_2(^{\bullet}\text{OH}) \underset{\text{Products}}{\overset{k_{23}\ \text{dye}}{\longrightarrow}} \text{TiO}_2 \underset{k_{10}}{\overset{k_{01}\ h\nu}{\longleftrightarrow}} \text{TiO}_2(\text{h}^+)\, D_{11}$$
$$= k_{23}k_{01}IC \tag{13}$$

$$D_{22}: \text{TiO}_2\ (^{\bullet}\text{OH}) \underset{\text{Products}}{\overset{k_{23}\ \text{dye}}{\longrightarrow}} \text{TiO}_2 \underset{k_{10}}{\overset{k_{01}\ h\nu}{\longleftrightarrow}} \text{TiO}_2(\text{h}^+) \overset{k_{12}\text{H}_2\text{O}}{\underset{\text{H}^+}{\Longrightarrow}} \text{TiO}_2(^{\bullet}\text{OH}) D_{22}$$
$$= k_{01}k_{12}I \tag{14}$$

Combining Eqs. (11)–(14) leads to

$$-r_{\text{dye}} = -\frac{dC}{dt} = \frac{k_{01}k_{12}k_{23}IC[S_T]}{k_{12}k_{23}C + k_{10}k_{23}C + k_{23}k_{01}IC + k_{01}k_{12}I} \tag{15}$$

where I is the UV light intensity, C is the dye concentration, and $[S_T]$ is the total catalyst site concentration. The above rate equation for dye degradation can be reduced to the following form:

$$-r_{dye} = -\frac{dC}{dt} = \frac{k_aC}{1 + k_bC} \tag{16}$$

where the lumped parameters are defined as

$$k_a = k_{23}[S_T], \quad k_b = \frac{k_{23}(k_{12} + k_{10} + k_{01}I)}{k_{01}k_{12}I} \tag{17}$$

In the dye degradation experiments conducted with the same UV lamp in the same photoreactor, k_a and k_b are constant. Thus, integrating Eq. (16) with initial condition: at $t = 0$, $C = C_0$ leads to

$$t = \frac{k_b}{k_a}C_0\left(1 - \frac{C}{C_0}\right) - \frac{1}{k_a}\ln\frac{C}{C_0} \tag{18}$$

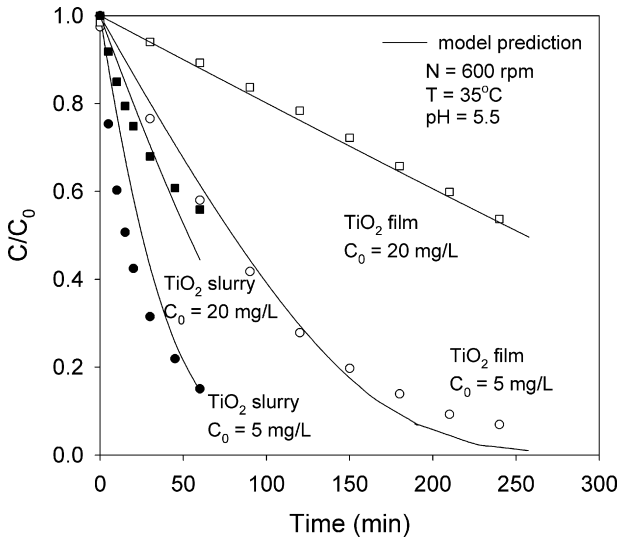

Fig. 11. Comparison of the dye degradation kinetic curves of the TiO_2 film and TiO_2 slurry systems.

The two lumped parameters can be obtained from fitting the experimental data to Eq. (18) using nonlinear regression and the results are $k_a = 0.0326\ \text{min}^{-1}$ and $k_b = 0.764\ \text{L mg}^{-1}$. As shown in Fig. 9, the developed kinetic model fits the experimental data satisfactorily. Using Eq. (18), the dye degradation conversion at any given time can be calculated by the developed kinetic model.

3.5. Comparison with TiO_2 slurry

Two dye degradation tests using $0.5\ \text{g L}^{-1}$ nano-sized TiO_2 suspension (Hombikat XXS100) were performed to compare with the performance of the immobilized TiO_2 catalysts. As is shown in Fig. 11, the dye degradation rate in the TiO_2 film system is lower than that in the TiO_2 slurry system. Because the total surface area in the TiO_2 slurry reactor is much higher than that in the TiO_2 film-coated photocatalytic reactor, the dye degradation rate is therefore higher in the TiO_2 slurry system. In spite of having a higher degradation rate, the TiO_2 catalyst cannot be recovered in the slurry system. To get a higher dye removal rate in the TiO_2 film-coated photocatalytic reactor, one needs to extend the reaction time or to use a larger photocatalytic reactor with a larger total catalyst site concentration $[S_T]$.

4. Conclusions

TiO_2 films were successfully immobilized onto the inner surface of cylindrical glass reactors by coating the commercial nano-size TiO_2 suspension in the reactor at 50 rpm rotation speed for 50 min, followed by drying at 250 °C. The experimental results of a full factorial design indicate that the main effects of the rotation time, rotation speed, and drying temperature on the dye removal rate are significant. The dye removal rate decreases with increasing drying temperature at the shorter rotation time or lower rotation speed while it increases with increasing drying temperature at the longer rotation time or higher rotation speed. The dye degradation kinetics could not be adequately described by the first-order kinetic model. A new kinetic model, based on the proposed reaction mechanism has been developed to fit the kinetic data satisfactorily.

Acknowledgment

The financial support from Yonglin Foundation to Pei-Jen Lu is highly appreciated.

References

[1] Y. Anjaneyulu, N.S. Chary, D.S.S. Raj, Decolourization of industrial effluents—available methods and emerging technologies—a review, Rev. Environ. Sci. Biotechnol. 4 (2005) 245–273.
[2] A.E. Nemr, O. Abdelwahab, A. El-Sikaily, A. Khaled, Removal of direct blue-86 from aqueous solution by new activated carbon developed from orange peel, J. Hazard. Mater. 161 (2009) 102–110.
[3] V. Dulman, S.M. Cucu-Man, Sorption of some textile dyes by beech wood sawdust, J. Hazard. Mater. 162 (2009) 1457–1464.
[4] B.H. Hameed, Spent tea leaves: a new non-conventional and low-cost adsorbent for removal of basic dye from aqueous solutions, J. Hazard. Mater. 161 (2009) 753–759.
[5] B. Benguella, A. Yacouta-Nour, Adsorption of Bezanyl Red and Nylomine Green from aqueous solutions by natural and acid-activated bentonite, Desalination 235 (2009) 276–292.
[6] P. Leechart, W. Nakbanpote, P. Thiravetyan, Application of 'waste' wood-shaving bottom ash for adsorption of azo reactive dye, J. Environ. Manage. 90 (2009) 912–920.
[7] U.R. Lakshmi, V.C. Srivastava, I.D. Mall, D.H. Lataye, Rice husk ash as an effective adsorbent: evaluation of adsorptive characteristics for Indigo Carmine dye, J. Environ. Manage. 90 (2009) 710–720.
[8] A.L. Barros, T.M. Pizzolato, E. Carissimi, I.A.H. Schneider, Decolorizing dye wastewater from the agate industry with Fenton oxidation process, Miner. Eng. 19 (2006) 87–90.
[9] J.-H. Sun, S.-P. Sun, G.-L. Wang, L.-P. Qiao, Degradation of azo dye Amido black 10B in aqueous solution by Fenton oxidation process, Dyes Pigments 74 (2007) 647–652.
[10] N. Modirshahla, M.A. Behnajady, F. Ghanbary, Decolorization and mineralization of C.I. Acid Yellow 23 by Fenton and photo-Fenton processes, Dyes Pigments 73 (2007) 305–310.
[11] C.-H. Wu, C.-Y. Kuo, C.-L. Chang, Decolorization of azo dyes using catalytic ozonation, React. Kinet. Catal. Lett. 91 (2007) 161–168.
[12] A. de, O. Martins, V.M. Canalli, C.M.N. Azevedo, M. Pires, Degradation of pararosaniline (C.I. Basic Red 9 monohydrochloride) dye by ozonation and sonolysis, Dyes Pigments 68 (2006) 227–234.
[13] M.A. Behnajady, H. Modirshahla, Fathi, Kinetics of decolorization of an azo dye in UV alone and UV/H_2O_2 processes, J. Hazard. Mater. B136 (2006) 816–821.
[14] H.-Y. Shu, Degradation of dyehouse effluent containing C.I. Direct Blue 199 by processes of ozonation, UV/H_2O_2 and in sequence of ozonation with UV/H_2O_2, J. Hazard. Mater. B133 (2006) 92–98.
[15] I. Peternel, N. Koprivanac, H. Kusic, UV-based processes for reactive azo dye mineralization, Water Res. 40 (2006) 525–532.
[16] S.G. Schrank, J.N.R. dos Santos, D.S. Souza, E.E.S. Souza, Decolourisation effects of Vat Green 01 textile dye and textile wastewater using H_2O_2/UV process, J. Photochem. Photobiol. A-Chem. 186 (2007) 125–129.
[17] W.A.-A. Sadik, A.W. Nashed, UV-induced decolourization of acid alizarine violet N by homogeneous advanced oxidation processes, Chem. Eng. J. 137 (2008) 525–528.
[18] L. Wojnárovits, E. Takács, Irradiation treatment of azo dye containing wastewater: an overview, Radiat. Phys. Chem. 77 (2008) 225–244.
[19] E. Chatzisymeon, N.P. Xekoukoulotakis, A. Coz, N. Kalogerakis, D. Mantzavinos, Electrochemical treatment of textile dyes and dyehouse effluents, J. Hazard. Mater. B137 (2006) 998–1007.
[20] Z. Zainal, C.Y. Lee, M.Z. Hussein, A. Kassim, N.A. Yusof, Electrochemical-assisted photodegradation of mixed dye and textile effluents using TiO_2 thin films, J. Hazard. Mater. 146 (2007) 73–80.
[21] N. Bensalah, M.A. Quiroz Alfaro, C.A. Martinez-Huitle, Electrochemical treatment of synthetic wastewaters containing Alphazurine A dye, J. Chem. Eng. 149 (2009) 348–352.
[22] C.A. Martínez-Huitle, E. Brillas, Decontamination of wastewaters containing synthetic organic dyes by electrochemical methods: a general review, Appl. Catal. B-Environ. 87 (2009) 105–145.
[23] M.H. Habibi, N. Talebian, Photocatalytic degradation of an azo dye X6G in water: a comparative study using nanostructured indium tin oxide and titanium oxide thin films, Dyes Pigments 73 (2007) 186–194.
[24] M. Muruganandham, M. Swaminathan, Solar driven decolourisation of Reactive Yellow 14 by advanced oxidation processes in heterogeneous and homogeneous media, Dyes Pigments 72 (2007) 137–143.
[25] E.R. Bandala, M.A. Peláez, A.J. García-López, M. de, J. Salgado, G. Moeller, Photocatalytic decolourisation of synthetic and real textile wastewater containing benzidine-based azo dyes, Chem. Eng. Process. 47 (2008) 169–176.
[26] C.-H. Wu, H.-W. Chang, J.-M. Chern, Basic dye decomposition kinetics in a photocatalytic slurry reactor, J. Hazard. Mater. B137 (2006) 336–343.
[27] M.O. Abou-Helal, W.T. Seeber, Preparation of TiO_2 thin films by spray pyrolysis to be used as a photocatalyst, Appl. Surf. Sci. 195 (2002) 53–62.
[28] B.-H. Kim, J.-Y. Lee, Y.-H. Choa, M. Higuchi, N. Mizutani, Preparation of TiO_2 thin film by liquid sprayed mist CVD method, Mater. Sci. Eng. B107 (2004) 289–294.
[29] E. Gressel-Michel, D. Chaumont, D. Stuerga, From a microwave flash-synthesized TiO_2 colloidal suspension to TiO_2 thin films, J. Colloid Interface Sci. 285 (2005) 674–679.
[30] T. Miyata, S. Tsukada, T. Minami, Preparation of anatase TiO_2 thin films by vacuum arc plasma evaporation, Thin Solid Films 496 (2006) 136–140.
[31] B.-H. Kim, J.-H. Ahn, J.-H. Jeong, Y.-S. Jeon, K.-O. Jeon, K.-S. Hwang, Preparation of TiO_2 thin film on SiO_2 glass by a spin coating–pyrolysis process, Ceram. Int. 32 (2006) 223–225.
[32] A.R. Rao, V. Dutta, Low-temperature synthesis of TiO_2 nanoparticles and preparation of TiO_2 thin films by spray deposition, Sol. Energy Mater. Sol. Cells 91 (2007) 1075–1080.
[33] F.L. Toma, L.M. Berger, D. Jacquet, D. Wicky, I. Villaluenga, Y.R. de Miguel, J.S. Lindeløv, Comparative study on the photocatalytic behaviour of titanium oxide thermal sprayed coatings from powders and suspensions, Surf. Coat. Technol. 203 (2009) 2150–2156.
[34] P. Rodriguez, V. Meille, S. Pallier, M.A.A. Sawah, Deposition and characterisation of TiO_2 coatings on various supports for structured (photo)catalytic reactors, Appl. Catal. A: Gen. 360 (2009) 154–162.
[35] M. Uzunova-Bujnova, R. Todorovska, M. Milanova, R. Kralchevska, D. Todorovsky, On the spray-drying deposition of TiO_2 photocatalytic films, Appl. Surf. Sci. 256 (2009) 830–837.
[36] E. Stathatos, P. Lianos, C. Tsakiroglou, Metachromatic effects and photodegradation of basic blue on nanocrystalline titania films, Langmuir 20 (2004) 9103–9107.
[37] E. Stathatos, P. Lianos, C. Tsakiroglou, Highly efficient nanocrystalline titania films made from organic/inorganic nanocomposite gels, Micropor. Mesopor. Mater. 75 (2004) 255–260.
[38] H. Choi, E. Stathatos, D.D. Dionysiou, Sol-gel preparation of mesoporous photocatalytic TiO_2 films and TiO_2/Al_2O_3 composite membranes for environmental applications, Appl. Catal. B: Environ. 63 (2006) 60–67.
[39] H. Choi, E. Stathatos, D.D. Dionysiou, Photocatalytic TiO_2 films and membranes for the development of efficient wastewater treatment and reuse systems, Desalination 202 (2007) 199–206.
[40] Y. Chen, E. Stathatos, D.D. Dionysiou, Microstructure characterization and photocatalytic activity of mesoporous TiO_2 films with ultrafine anatase nanocrystallites, Surf. Coat. Technol. 202 (2008) 1944–1950.
[41] Y. Chen, E. Stathatos, D.D. Dionysiou, Sol–gel modified TiO_2 powder films for high performance dye-sensitized solar cells, J. Photochem. Photobiol. A: Chem. 203 (2009) 192–198.
[42] G.E.P. Box, W.G. Hunter, J.S. Hunter, Statistics for Experimenters, John Wiley & Sons, New York, 1978.
[43] O. Levenspiel, Chemical Reaction Engineering, 3rd ed., John Wiley & Sons, New York, 1999.
[44] A. Fujishima, T.N. Rao, D.A. Tryk, Titanium dioxide photocatalysis, J. Photochem. Photobiol. C: Photochem. Rev. 1 (2000) 1–21.
[45] C. Galindo, P. Jacques, A. Kalt, Photodegradation of the aminoazobenzene acid orange 52 by three advanced oxidation processes: UV/H_2O_2, UV/TiO_2 and VIS/TiO_2: comparative mechanistic and kinetic investigations, J. Photochem. Photobio. A: Chem. 130 (2000) 35–47.
[46] M.H. Habibi, A. Hassanzadeh, S. Mahdavi, The effect of operational parameters on the photocatalytic degradation of three textile azo dyes in aqueous TiO_2 suspensions, J. Photochem. Photobiol. A: Chem. 172 (2005) 89–96.
[47] J.M. Chern, General rate equation and their application for cyclic reaction networks: single-cycle systems, Ind. Eng. Chem. Res. 39 (2000) 4100–4105.